Airborne Observations of an Asteroid Entry for High Fidelity Modeling: Space Debris Object WT1190F

Peter Jenniskens[1], Jim Albers[2], Michael W. Koop[2]
SETI Institute, Mountain View, CA 94043, U.S.A.

Mohammad S. Odeh[3], Khalfan Al-Noimy[4]
International Astronomical Center, Abu Dhabi, United Arab Emirates

Khalfan Al-Remeithi[5], Khaled Al Hasmi[6]
UAE Space Agency, Abu Dhabi, United Arab Emirates

Ronald F. Dantowitz[7]
Dexter Southfield, Brookline, MA 02445, U.S.A.

Forrest Gasdia[8]
Embry-Riddle Aeronautical University, Daytona Beach, FL 32114, U.S.A.

Stefan Löhle[9], Fabian Zander[10], Tobias Hermann[10]
Universität Suttgart, D-70569 Stuttgart, Germany

Davide Farnocchia[11], Steve R. Chesley[12], Paul W. Chodas[11], Ryan S. Park[11], Jon D. Giorgini[11]
Jet Propulsion Laboratory/California Institute of Technology, Pasadena, CA 91109, U.S.A.

William J. Gray[13]
Bowdoinham, ME 04008, U.S.A.

Darrel K. Robertson[14]
NASA Ames Research Center, Moffett Field, CA 94035, U.S.A.

and

Tobias Lips[15]
Hypersonic Technology Göttingen, D-37191 Katlenburg-Lindau, Germany

[1] Senior Research Scientist, Carl Sagan Center, 189 Bernardo Ave, AIAA Member.
[2] SETI Institute Volunteer, 189 Bernardo Ave, No AIAA Member.
[3] Director, P. O. Box 41353, No AIAA Member.
[4] President, P.O. Box 41353, No AIAA Member.
[5] Manager, P. O. Box 7133, No AIAA Member.
[6] Director Space Missions Management, P.O. Box 7133, No AIAA Member.
[7] Director, Clay Center Observatory, 20 Newton Street, AIAA Member.
[8] Master's Student, 600 S. Clyde Morris Blvd., No AIAA Member.
[9] Research Scientist, High Enthalpy Flow Diagnostics Group leader, Institut für Raumfahrtsysteme, Pfaffenwaldring 31, AIAA Member.
[10] Post-Doc and Ph.D. student, respectively, High Enthalpy Flow Diagnostics Group, Institut für Raumfahrtsysteme, Pfaffenwaldring 31, AIAA Member.
[11] Navigation Engineer, Center for Near Earth Object Studies, 4800 Oak Grove Dr., No AIAA Member.
[12] Senior Research Scientist, Center for Near Earth Object Studies, 4800 Oak Grove Dr., No AIAA Member.
[13] Programmer, 168 Ridge Road, No AIAA Member.
[14] Research Engineer, Asteroid Threat Assessment Project, Mail Stop 258-6, AIAA Member.
[15] Managing Director, Albert-Einstein Str. 11, No AIAA Member.

First results are presented from an airborne observing campaign that practiced the study of a future announced small-asteroid entry to support high-fidelity asteroid impact modeling. On November 13, 2015, space debris object WT1190F returned to Earth on an eccentric orbit with an entry speed of 10.61 km/s, relative to the atmosphere at 100 km altitude, and an entry angle of 20.6º. These circumstances are more similar to those of asteroid impacts than to most other space debris re-entries. The unusual entry also offered an opportunity to validate space debris re-entry safety models. In the days leading up to the event, the time and position of the re-entry were refined from astronomical observations. It was found that the object was spinning rapidly with a period of 1.5s. Expected spectral signatures and mechanical and thermal stresses were modeled based on an assumed nature of the object. The International Astronomical Center in Abu Dhabi and the United Arab Emirates Space Agency deployed an instrumented G450 aircraft to observe the daytime re-entry over the Indian Ocean just south of Sri Lanka. The entry was successfully observed and documented by video and spectrographic cameras. A light curve was measured. The main fragmentation event occurred at 55.8 ± 2.5 km altitude. The object produced TiO molecular emission bands and hydrogen alpha emission during a disruption of one of the fragments. Two fragments were observed to survive down to at least 33-km altitude, where they left the field of view. With lessons learned, a future rapid response observing campaign to study a natural asteroid impact is feasible, even in daytime conditions, if sufficient warning time is provided.

Nomenclature

q	=	perihelion distance	e	=	eccentricity
i	=	inclination	TDB	=	Barycentric Dynamical Time
Q	=	aphelion distance			

I. Introduction

ANNOUNCED small (few-m sized) asteroid impacts are uniquely suited for validating asteroid impact models. Such models address the process of fragmentation, which dictates at which altitude the kinetic energy of an asteroid is deposited. To evaluate the potential for causing damaging airbursts,[1–2] high fidelity modeling requires a known size, mass, shape, entry orientation, entry speed, entry angle, time and location of entry, as well as material properties of the impacting asteroid. While an announced small asteroid is on approach, information on the pre-impact shape, orientation, orbit, and material properties can be gathered from astrometry, photometry, light curves, spectra, and radar observations, amongst others. If sufficient warning time is available, the atmospheric entry can be observed to document the fragmentation sequence. After the entry, surviving samples can be collected on the ground in the form of meteorites or, over the ocean, as dust in airborne collections.

One-meter sized asteroids impact Earth about once a week from the nighttime side of Earth, while 4-meter sized asteroids impact about once a year.[2–3] If discovered at apparent +21 magnitude, there would be only about 1 and 4 days of warning, respectively. A once per five year 7-m sized asteroid would provide at best ~7 days of warning, the warning time being about proportional to diameter.[4]

So far, only asteroid 2008 TC_3 was observed in space, 20 hours prior to impact, characterized, and then recovered in part as meteorites on the ground.[5] The entry was observed by geostationary weather satellites in October of 2008,[6] but no time-resolved data of the entry are publicly available. A second about 4-m diameter asteroid, 2014 AA, was discovered 21 hours before impact but no characterization was obtained prior to impact.[7]

A detailed study of the next TC3-like impact would require an airborne observing campaign to be mounted at short notice. Close to 70% of all asteroid impacts on Earth occur over the ocean and half are in daytime. Hence, small asteroid impact observations require an instrumented airborne platform, capable to work both in daytime and nighttime, to take a multi-disciplined research team to the right location at the right time. From a safe 100–300 km distance, the impact would be low enough in the sky to be seen from the aircraft windows.

Such observations could set constraints on radiative heating, ablation rate, and fragmentation processes from measuring the air plasma emission escaping the shock, elemental atom line emissions and excitation conditions, pressure broadening, and deceleration in the plane of the known trajectory.[8-12] It is also possible to measure wake,

light curve and air plasma emission line intensities early in flight that can be used to evaluate the presence of regolith and the internal cohesion of asteroids. The main element abundance (asteroid composition) can be measured for individual fragments, while CN-band emission can point to the presence of organic matter, for example.[16] Such information will help constrain the meteorite type if no meteorites can be recovered in an over-the-ocean impact (e.g., ordinary chondrites with low or high iron content). The observed altitude of disruption can be used to direct airborne dust collection efforts in the atmosphere.

To prepare for such airborne observing campaign and facilitate the quick and pristine recovery of meteorites, an international "Next TC3 Consortium" was established in 2014.[16] The Consortium brought together the observers most likely to detect an imminently impacting asteroid, the dynamicists capable of evaluating the sparse early observations and provide early warning for interesting close approaches and potential impactors,[13] the observers that would characterize the asteroid's shape and spin states in space, and the airborne observers set to study the entry and recover meteorites.

On October 3, 2015, an opportunity arose that offered the best possible practice for all aspects of such an observing campaign. An object was discovered as a possible asteroid by the Catalina Sky Survey (CSS) in Tucson, Arizona, and was quickly identified as an artificial object in an eccentric (e = 0.94) orbit with respect to Earth. It was given the designation WT1190F, with letters and numbers reflecting the time, instrument and sequence of detection, respectively (Fig. 1).[17] It was then found that this object was previously observed in February of 2013 (designated UDA34A3) and in late November 2013 (UW8551D). Taken together, the forward integrated orbit implied that the object would impact Earth with a speed of ~11 km/s and entry angle ~20º near the coast of Sri Lanka at 06:18 UT on Friday November 13, 2015. This would be the first predicted impact of space debris on such an eccentric asteroid-like orbit (Fig. 2).

The similarity to the impact of natural asteroids, and the desire to study the behavior of re-entering space debris at such high entry speed and angle, suggested the organization of an observing campaign to document the manner in which this object fragments in the atmosphere in challenging daytime conditions.

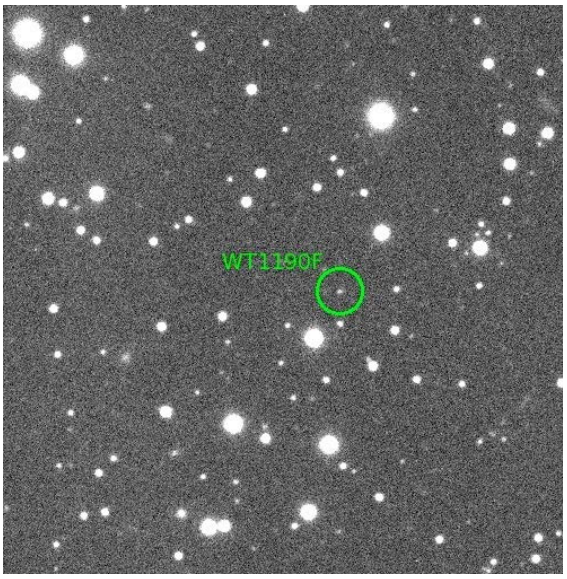

Figure 1. WT1190F on approach to Earth. *Magdalena Ridge Observatory detection of WT1190F at apogee on November 3, 2015, in an image by Bill Ryan (with permission).*

Figure 2. Final orbit of WT1190F in the days leading up to the re-entry. *The orbit of the Moon marks the scale. View is from the South Pole.*

II. Pre-entry observations

A. Pre-entry astronomical observations

The pre-entry orbit was determined based on 800 observations starting Nov. 4 and running up to 05:44 UT Nov 13, half an hour before re-entry. At the Epoch of 2015 Nov. 13.267820 TDB, the object had a geocentric inclination of i = 13.24848 ± 0.00003º in an equatorial coordinate system, with perihelion at q = 5,731.36 ± 0.03 km and

[16] *Jenniskens, P., "Next TC3 Consortium", Website http://impact.seti.org (last viewed November 16, 2015), 2015.*
[17] *Gray, W. J., "WT1190F FAQs", Website http://projectpluto.com/temp/wt1190f.htm (last viewed November 16, 2015), 2015.*

aphelion at Q = 607,765 ± 3 km, a distance of about 1.6 times that of the Moon.[18] The orbital period at that time was 19.57d. The object would enter Earth's atmosphere at 100 km altitude over +6.1594ºN latitude and 79.0757ºE longitude, with an apparent speed of 10.606 km/s relative to the observer, after extrapolating the Earth rotation to the atmosphere at 100 km altitude, and an entry angle relative to the local horizon of 20.64º. The accuracy of this result was mainly from accurate, well-timed data in the hours prior to re-entry. Without the large set of (Z66) DeSS Deimos Sky Survey data, the 100-km altitude point would shift 0.31-s earlier, 650-m north, and 1.4-km westward.

The absolute magnitude was H = 31.2 ± 0.1 magn., which corresponds to a size of about 1.5-m, for an assumed albedo of 25%.[14] The trajectory model suggests an average surface-to-mass ratio of 0.01176 ± 0.00045 m^2/kg, being variable with an amplitude larger than the uncertainty quoted. A spherical model implied a mass of 50–200 kg.

Previously, the objects designated UW8551D and UDA34A3 were recognized to be the same.[18] The new dynamical link of these to WT1190F established its orbit. Forward integration showed that this object would orbit the Earth one more time, then impact on November 13, 2015, off the coast of Sri Lanka.

This also set the stage for linking WT1190F to previous observations. M. Micheli (NEO Coordination Centre, ESA) found the object in PanSTARRS observations from December 2012. P. Birtwhistle, an U.K. amateur astronomer, had suggested that the 2013 objects could be the same as an object observed in late 2009 and early 2010 called 9U01FF6. E. Christensen of CSS identified additional observations on 2011 January 5. Then Micheli found six detections in PanSTARRS based on the new ephemeris, three of which were in April of 2011 past a close lunar flyby. This enabled linking the June 2009 observations to the new object. At the time, the object was in a highly inclined i ~ 61º orbit.[17]

The calculation of a precise impact location and time required a good understanding of the outward solar radiation pressure force on the object, which varied as a function of the object's shape, albedo, and orientation. Leading up to the impact, the object had not yet been positively identified to assist in evaluating these forces. To mitigate for these modeling issues the data arc was shortened as the object approached Earth for the final re-entry.

In the hour before entry, P. Birtwhistle at Shefford Observatory, U.K., obtained trailed images of WT1190F when the object was bright and moving fast. Those images showed a 1.48-s modulation in brightness, consisting of a bright flash followed by a fainter flash.[19] There was no sign of non-principal axis rotation.

B. Pre-entry model calculations

To better understand the expected duration and peak brightness of the object, as well as its spectroscopic signatures, various aspects of the entry were modeled using pre-existing object models or an assumed shape. At the Institut für Raumfahrtsysteme, the expected radiation signature for a spherical object entering at the expected speed were calculated for altitudes of 80 and 43 km using the URANUS flowfield solutions and PARADE spectral simulations.[15] The calculations show significant air plasma emissions, both O, N lines at wavelengths 742–873 nm and strong N_2^+ emission bands below 400 nm. The spectral radiance of the OI line at 777 nm (at the spectral resolution of the Echelle spectrograph deployed during the mission) reached 4.6×10^4 and 1.0×10^4 W/m^2/nm/sr at 80 and 43 km, respectively. At a distance of 300 km, the OI air plasma irradiation would be ~10^{-11} W/m^2/nm.

At Hypersonic Technology Göttingen, the entry was modeled using the SCARAB software,[16] assuming that WT1190F was a Delta-II Second Stage rocket (the main component of which is a stainless steel tank). The model has an area-to-mass ratio of about 0.01 m^2/kg. Thermal stresses were evaluated. The relatively high entry speed was found to delay the heat penetrating vulnerable structures, as a result of which main fragmentation was expected to be delayed compared to a more shallow re-entry. The first breakup was expected at about 60-km altitude. It takes only 17 s to travel from 122 km (SCARAB re-entry interface; 10.6 km/s) down to 60 km, where the velocity had decreased to 10.4 km/s. After another 14 s, the object had travelled from 60 km down to 29 km (Mach 6 limit, 1.8 km/s), at which time the object would no longer be radiating brightly. This implied an observing time of less than 30 s. The biggest surviving object took another ~250 s before impacting at about 71 m/s. In this model, two thirds of the initial mass survived the re-entry.

At NASA Ames, the mechanical stresses during entry were modeled based on a stylized PAM-D Payload Assist Module model, mainly composed of a titanium tank and a carbon phenolic nozzle, using methods applied also to small asteroid impact models.[17] The empty PAM-D has a surface-to-mass ratio of about 0.005-0.007 m^2/kg. It was found that a titanium tank would nearly completely survive, even under these high entry speed and entry angle conditions. Due to the low density, the object decelerated rapidly to terminal velocity and the shock-heated surface temperature rapidly dropped below the melting point.

---

[18] Gray, W. J., "Pseudo-MPEC for UDA34A3 = UW8551D = WT1190F", Website http://projectpluto.com/temp /mpec_all.htm (last viewed November 16, 2015), 2015.

[19] Birtwhistle, P., "Inside Great Shefford Observatory", Website http://peter-j95.blogspot.com/ (last viewed 11/16/2015), 2015.

III. Airborne observations

An observing campaign was organized by the International Astronomical Center (IAC) in Abu Dhabi and the United Arab Emirates (UAE) Space Agency. The UAE is located at a relatively short deployment distance from the impact location near Sri Lanka. A G450 business jet was chartered to bring a research team to a location over the Indian Ocean, just south of the trajectory in order to keep the near-noon Sun behind the observers. There would be a refuel stop at Columbo in Sri Lanka before returning home.[20]

An experienced team of re-entry observers[18–21] was invited to participate. To enable high-resolution imaging, the protective pane from the front two of the five aircraft windows was removed. A GPS antenna was placed in the cockpit window, which recorded the position of the aircraft as a function of time (Fig. 3).

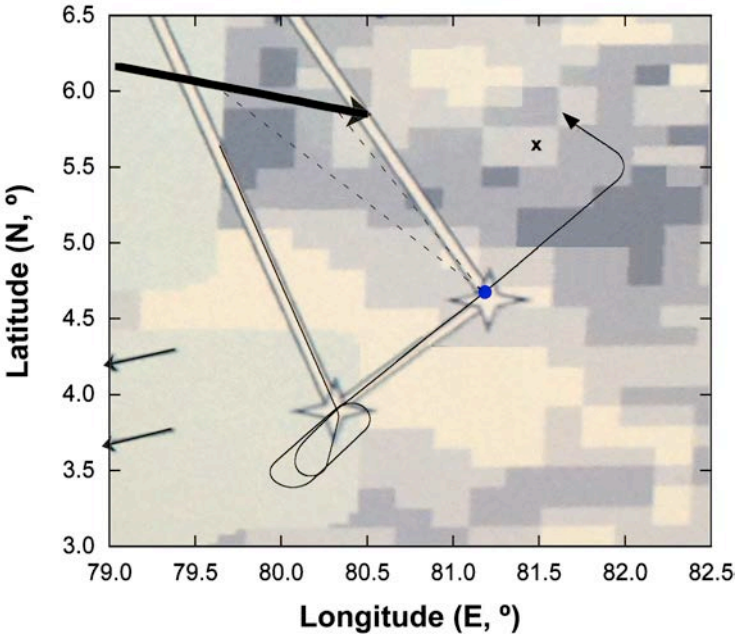

Figure 3. Aircraft route relative to WT1190F trajectory (thick arrow). *Any debris would have fallen well West of the "x", which marks the impact point if there was no atmosphere. The background shows the latest weather map update at 05 UT, with white showing clouds above 12,500 m, dark gray below 6,100 m. The parallel thin arrows mark the wind direction. The aircraft first settled into a racetrack pattern before embarking on the observing leg. By the time of entry (blue point), an approaching clearing had reached the site.*

From front to back, the instrument teams included a team from Dexter-Southfield Schools and Embry-Riddle Aeronautical University. They operated a *Red EPIC* movie camera equipped with a 200-mm focal length lens. The camera was mounted on a *Gizmo* ballmount attached to a *Pelican* hard case, strapped inside the seat in front of the window. The camera was hand-tracked using an *i-glasses* VIDEO video head mounted display and a 20 x 30º field-of-view *Watec* Wat 902H2 Ultimate pointing camera with a near-IR filter to bring out the object from the background sky. The camera also contained two *Prosilica* monochrome spectrographic cameras (1360 x 1040 pixels at 6.45 micron/pixel), run at 30 frames/s and 14-bit depth, with a 50-mm focal length lens. To accomplish slit-less spectroscopy in daytime conditions, two techniques were applied. One red spectrograph used a short exposure (150 μs) and high F-number (F16) to suppress the background. This spectrograph was equipped with a 300 l/mm grating and a measured dispersion of 0.413±0.004 nm/pixel. A second blue spectrograph (< 500 nm) pointed at a dark surface to suppress the zero-order image, and was equipped with a 1200 l/mm grating for a nominal dispersion of 0.086 nm/pixel.

A second clear window was used by the IAC team to operate a second *Red EPIC* camera equipped with 100-mm focal length F8 lens (exposure time 1/4000th s), operated at 120 frames per second and put slightly out of focus for high precision photometry. The camera was also mounted on a *Gizmo* ball mount and *Pelican* suitcase. The same pointing camera with near-IR filter and a video headset display were used to enable hand tracking. A co-mounted spectrograph with 1200 l/mm was overexposed by low clouds and did not return data.

The third window was used by the SETI Institute team, deploying a number of staring cameras with the purpose to collect data if the pointed cameras would fail. This included a *Sony* α7s digital camera with F1.8/55 mm lens and operated at 1/160s F4 in imaging mode and 60i (60 frames per second) in video mode. In addition, eight *Watec* Wat902 H2 Ultimate cameras equipped with 394, 512, 654, and >800 nm narrow band filters for photometry were recorded at 15 frame/s on a video security camera Digital Video Recorder (DVR). Two cameras were set up for spectroscopy, using 1200 l/mm gratings, one with a long pass filter for red wavelengths, the other looking at a dark surface for blue wavelengths. The two remaining cameras were set up with neutral density filters and aimed sideways to cover a larger part of the sky. All cameras had a ~20 x 30º field of view. A staring *GoPro* Hero 3

[20] *For more information: http://impact.seti.org; https://youtu.be/YJT-q8_dl88*

camera and an optical acoustic sensor were mounted co-aligned in this window. Also, a wide angle *GoPro* camera and a *Lumix* camera were installed in the cockpit to cover an area of sky with a more forward view.

The fourth window was occupied by an IAC-owned 60-mm focal length *Lumenera* monochrome camera on a ball mount, and was operated by the UAE Space Agency team. The camera was also equipped with a spotting camera and a video headset display to point the instrument at the meteor.

The fifth and final window was used by the University of Stuttgart team to point collection optics at the entry for collecting light in an optical fiber to supply a small Echelle spectrograph for high-resolution spectroscopy at 380–880 nm wavelengths. The instrument was composed of two co-aligned cameras for broadband photometry and a *Sony* camcorder for simple visual impression video. A video headset display was used for pointing, but the object was acquired late because lack of reference in the clouded sky caused the observers to aim too low in the sky for acquisition.

Figure 4. Wide-field view of the WT1190F re-entry. *The object moved from top left to bottom right towards the observer. The field of view is about 17º x 30º (Sony α7s).*

The flight path was designed so that the aircraft was downrange, offering as much as possible a view of the hot front area of the object. This would facilitate the interpretation of the data in case the object stayed intact, as was the case for the Stardust and Hayabusa capsules.[20-21]

Weather was the challenging factor. Ground-based observations from Sri Lanka were hampered by rain. The clouds just south of the island were also frequently well above the ceiling of the flight altitude (Fig. 3). A flight path was designed to time the arrival of the aircraft in a small low-cloud (<6,100 m) area at the predicted time of the entry (Fig. 3), slightly further down range than originally planned. The entry was observed when the aircraft was at a position +4.6670 ºN, 81.1833 ºE, at an altitude of 14,439 m (Fig. 3).

From that viewing point, the meteor was expected to pass the 100-km point at 06:18:21.72 UT in a direction 15.7º above the horizon at 306 km distance, pass the 75-km point at 06:18:28.49 UT in a direction 14.5º above the horizon at 241 km, and pass the 40-km altitude point at 06:18:39.24 UT in a direction of 10.4º elevation at 154 km distance, causing a slightly downward sloped path in the sky (Fig. 4).

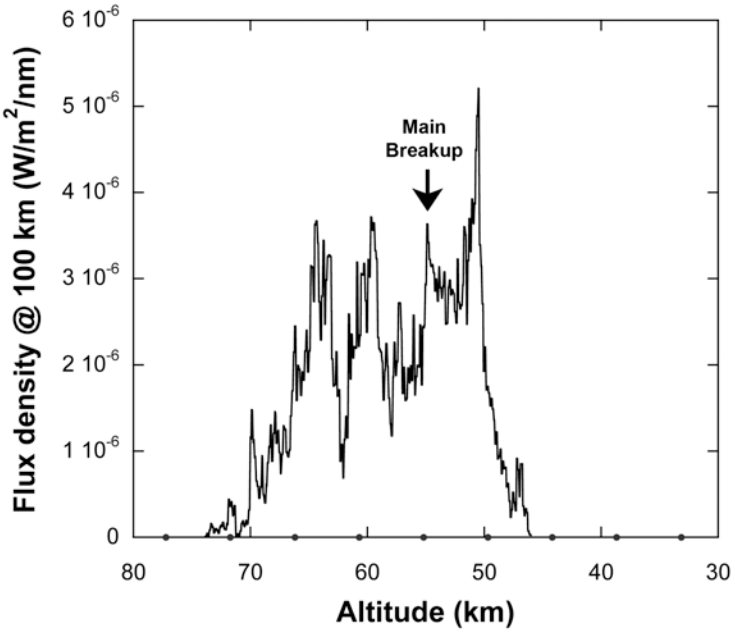

Figure 5. Visible-band light curve. *The altitude scale in this Sony α7s data follows from a ballistic trajectory with coefficient 0.01 kg/m². Dots near the bottom mark a periodic 1.48s spin period.*

IV. Results

The entry was observed successfully (Fig. 4). A first report was compiled onboard the aircraft on the way home and distributed as a *YouTube* video upon landing back in Abu Dhabi. The following section outlines preliminary results inferred form the observations in the weeks after the re-entry. This report was compiled following a partial data analysis. The conclusions may be refined once more data are analyzed.

A. Time, altitude and light curve

The time of re-entry (when passing the 100-km altitude point) was calculated from the pre-impact observations of WT1190F as 06:18:21.72 ± 0.03 s UT, based on 1480 measurements made between Oct. 22 and Nov. 12. Model-dependent systematic uncertainties can arise from differences in the force model used, the weighing of observations, and how timing issues are handled. The calculation was repeated with independent software packages, and by testing different data arcs with different weighting schemes. Care was taken to evaluate timing at the observatories. The result was in good agreement, finding an impact time of 06:18:21.60 ± 0.10 UT, based on 800 observations (Nov. 4 – 13).

Such a precision made it possible to correlate the observed phenomena in time to altitudes along the atmospheric trajectory calculated from the object's path prior to entry. An uncertainty of ±0.03 s in entry time corresponds to a systematic error of ±0.1 km in altitude.

The light curve derived by placing an iris over the video images of the *Sony* α7s camera is shown in Figure 5. The flux density was corrected for range to the object by normalizing to a standard distance of 100 km. The altitude scale changes with the assumed peak time and ballistic coefficient.

Figure 6. Fragmentation of WT1190F. *These Red EPIC single frames were taken just after the main fragmentation event (top) and at peak brightness (bottom).*

Because it was not possible to tap directly into the roof-mounted GPS antenna, the NTP server equipment to supply accurate time to the computers and cameras was not functioning correctly. The backup video time inserter units were running, but this video data was not recorded, because the digital video recorder lost access to the recording drive 10 minutes prior to re-entry. This also prevented recording data from the filtered widefield imagers (The *GoPro* cameras on window 3 lost battery power 20 seconds prior to the re-entry, but both wide angle cockpit-mounted cameras did record the event).

Table 1. Time of peak brightness. *This corresponds to the time of disruption of the lower fragment component 0.1 s after the main breakup.*

Instrument	Time (UT)	+/- (s)	Notes
SETI *Sony* α7s	06:18:35.64	0.5	from time of writing to disk
UAE camera	06:18:36.23	1.0	from computer set time
DS Blue Spectrograph	06:18:35.22	0.5	from computer set time
IRS Camcorder	06:18:34:58	1.0	from audio count-down

Because of this, we have a ±0.7 s timing uncertainty in the observations. Data were recorded on computers and digital cameras that had an internal clock set by hand or set to internet clocks prior to the mission. Those were calibrated by taking images of a handheld GPS system shortly after the mission. Table 1 summarizes the derived time of peak brightness, corresponding to the fragmentation of the lower component seen in Fig. 6, immediately after the main body split in two. The time estimates are in reasonable agreement, from which we adopt a peak time of 06:18:35.4 ± 0.7 s UT. At that time, WT1190F had reached an altitude of 50.5 ± 2.5 km (Fig. 5).

Figure 7. Wake at peak brightness. *The vertical scale in this sky-subtracted Red EPIC frame is expanded x2.*

This is 13.7 (±0.7) seconds after passing the 100-km point. The entry was first detected by the *Sony* α7s camera when WT1190F was at an altitude of 73 km at 06:18:29.1 UT, while the final fragments left the field of view in the UAE camera at 06:18:41.0 UT, for a total duration of 11.9 s.

Although the object was quickly saturated in the long-focal length *Red EPIC* camera, the slightly out-of-focus IAC-operated *Red EPIC* 2 camera provided photometric data. Compared to a *Gigahertz-Optik 10W Quartz-halogen* calibration lamp (BN0-102-01) observed during tarmac calibration tests after the mission (diameter 20 mm, at distance 35.5-m from the camera), the lower fragment's peak brightness in a 1/60s frame corresponds to (at 100 km distance) a magnitude of -11.2 at blue wavelengths, -12.9 at green, and -14.3 at red wavelengths, corresponding to a flux density of 2.1×10^{-6}, 5.4×10^{-6}, and 1.0×10^{-5} W/m^2/nm, respectively. This corresponds to continuum emission with a graybody temperature of T = 3,030 ± 100 K from a relatively large ~100 m^2 surface area, possibly from solid particles.

The light curve in Fig. 5 translates to an integrated kinetic energy of $\sim 9 \times 10^9$ J (0.002 kt) and a pre-entry mass of ~160 kg, if we assume a luminous efficiency of 6% (to within a factor of 2–3).[10]

The cameras recorded a strong wake of ablation products, in a pattern that reflects the observed light curve (Fig. 7). Ablation and fragmentation correlate in time with the 1.48-s spin period (Fig. 5). Significant wake was produced from the moment of the main breakup. The wind-distorted smoke cloud was detected in *Sony* α7s data at least until 06:25:30 UT, when terrestrial clouds blocked the view.

Figure 8. Shortly after breakup lower fragment. *UAE camera.*

B. Details of the fragmentation

Up to 11 fragments were detected in the UAE camera (Fig. 8), most more or less in line with the initial trajectory. The number of detected fragments jumped from 1 to 6 starting at 55.8 (±2.5) km, the main fragmentation event, and then from 6 to 11 starting at 47.2 (±2.5) km altitude. The 200-mm *Red EPIC* camera detected up to 18 fragments shortly after the main fragmentation event (Fig. 6), some with a blue or red color rather than a yellow color.

Breakup started at 60.0 ± 2.5 km, when at least one trailing red fragment (Fig. 6) and one leading blue fragment (Fig. 8) were released.

During the main breakup event at 55.8 ± 2.5 km, the object split in two large fragments and a number of smaller. The lower large fragment subsequently disintegrated, causing peak brightness and a strong wake (Fig. 8). This fragment had a significantly deviating path from the previous trajectory, suggesting some amount of Δv when it broke off in the main breakup (Fig. 7). It continued to fragment aggressively further down and was soon lost (Fig. 9).

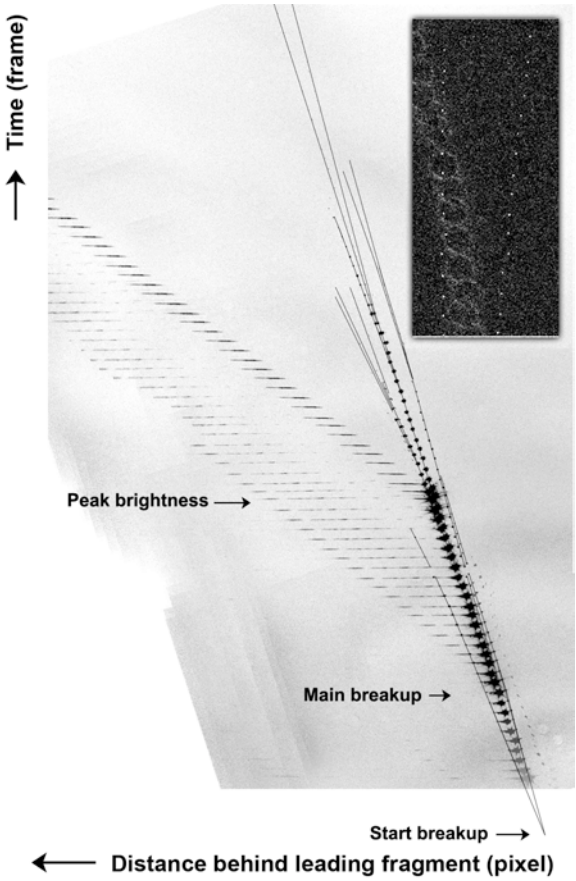

Figure 9. Fragment evolution. *In this UAE camera data composite, the relative position of fragments was aligned by hand and is shown at 15 frames/s intervals. The meteor moves from bottom to top. Inset shows the final frames (2x magnified).*

The upper large fragment survived longer in tact, and then continued to fragment, from which two pieces emerged that survived at least until they left the frame of view (Fig. 9, inset). The UAE camera tracked these objects until ~33 km altitude (this altitude is uncertain because the assumption of a constant surface-to-mass ratio of 0.01 m^2/kg may no longer apply). These two objects likely survived the entry to fall into the ocean.

The smaller fragments from the main breakup included one blue object and two side-by-side fragments with a distinct green core and red wake (Fig. 6). These two had a similar surface-to-mass ratio and ballistic coefficient, as one fragment gained on the other only slightly. Deceleration analysis will be required to determine if any of these fragments may have survived.

C. Composition

The red wavelength spectrograph recorded spectra when the radiation was most intense at the time of the disintegration of the lower object.

The spectra briefly showed a series of red-shaded molecular bands (Fig. 10). An emission line is visible as a dot towards the blue side of the spectrum in some frames, showing that the camera was well in focus.

The (in vacuum) wavelength scale was calibrated using emission line lamps. To obtain an absolute scale, the wavelength scale needs to be anchored to known emission lines or band heads.

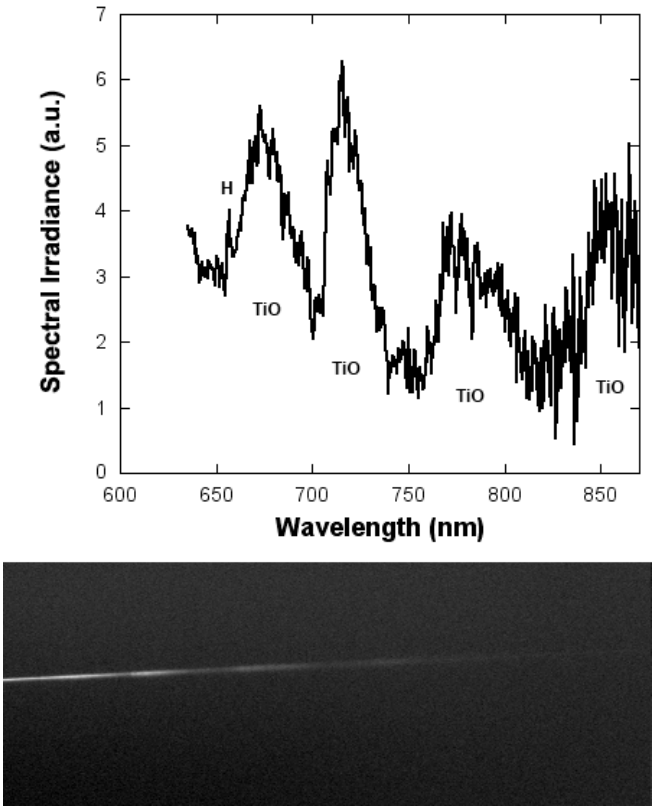

Figure 10. Slit-less spectrum from lower fragment at peak brightness. *Top: extracted spectrum after correction for instrument responsivity; Bottom: as observed.*

The bands are identified as the γ, γ', δ and ε molecular band systems of TiO, with excitation conditions similar to those seen in cool (~3000 K) stars.[22] If so, the emission line coincides with the 656-nm wavelength of the H_α line of hydrogen. During this disruption, no aluminum lines were detected in second order, which would show at 789–792 nm (Al I) in Fig. 10. Also, no strong air plasma emissions were observed at 777 nm (OI) and 822 nm (NI).

The upper fragment was also briefly detected in both spectrographs, well separated from the spectrum of the lower fragment. The upper fragment only showed a continuum emission at these wavelengths.

V. Discussion

A. Nature of WT1190F

There has been much speculation about the identity of this space debris object. The earliest available observations are from 2009 September 26, excluding missions after that date. Also, Monte-Carlo simulations of the orbital dynamics of WT1190F show a significant probability of either impacting Earth or the Moon on a 3–10-y timescale, making an origin during the Apollo period unlikely.

Any candidate body requires being able to produce the observed fragmentation sequence and the spectral signatures detected when the lower object disintegrated. Titanium and carbon phenolic surfaces would have resulted in continuum emissions when heated, except at the time of excessive ablation when titanium could produce TiO bands. The TiO bands could also have come from TiO_2-containing paint, but the emergence of hydrogen emission at the same time is consistent with some residual fuel and a titanium tank disruption, instead. The object did not strongly ablate aluminum at that time, although the blue fragments may have done so (causing AlO bands). If so, the Delta-II Second Stage is excluded as a candidate, on account of it having a stainless steel rather than a titanium tank.

One interpretation of the fragmentation sequence is that ablation and fragmentation occurred predominantly in a particular orientation of WT1190F. Once broken, the lower rapidly disintegrating fragment may be a component containing a titanium tank with residual fuel, explosively disrupting, while the upper fragment contained elements

that resisted ablation, perhaps including a carbon phenolic nozzle. It is not clear what are the two objects that survived in part to below 33 km altitude.

B. Models of WT1190F re-entry

With no certainty about the identification of this object at the time of writing, a direct comparison between models and observations is not possible. However, the entry did appear to show the expected delay of fragmentation due to the high entry speed. Fragmentation was observed to start at 60.0 ± 2.5 km, in agreement with the 60 km altitude predicted for a Delta-II Second Stage from SCARAB modeling. The observations also confirm the modeling result that fragments can survive the re-entry even under these relatively steep and fast entry conditions.

C. Lessons learned

The campaign was a good exercise for those involved in pre-impact observations and real-time impact location predictions. It was not good that weather hampered planned observations during the October 24 flyby. As a result, the fast rotation of the object was not resolved until it became bright enough for short exposures in the hours prior to impact. Obtaining accurate, well-timed astrometry shortly before impact dramatically improved the impact location and time predictions. A lesson we also saw with 2008 TC_3, where it helped tremendously that the object was well observed from Europe before it hit the Earth's shadow. In a future announced small asteroid impact, the area on Earth with best viewing of the object in the hours prior to impact should be identified early.

As far as the airborne observations are concerned, how does this observing campaign compare to a possible future announced small-asteroid impact observing campaign? For one, there was more time to bring the campaign together. In the case of WT1190F, there were 6 weeks between the first detection of the object on October 3 and the impact on November 13. Can this be compressed to a period of seven days? Possibly. In less than a week, funding was committed and transferred, an aircraft was chartered, and the aircraft operators received permission from Sri Lankan authorities for the commercial flight. That authorization was later challenged and it took another few days to have all parties involved agree to the flight plan. Potential delays of this nature are less likely if the impact is further from land. Also, several days were needed to obtain permission for this team to enter the Al Bateen airport to be able to work at the aircraft to set up the cameras. Such requirements are specific to the airport from which we can deploy.

Because of the large distance from San Francisco, travel to the United Arab Emirates took a day. Both U.S. and European teams arrived in the early morning of Nov. 11. It took a day and a half to set up the instruments in the aircraft. The main time-consuming part of the instrument installation was the adaptation of the camera position to the available seat geometry. For future campaigns a customized, variable seat mount can be developed which allows a mounting of cameras connected to the armrests for various aircraft seat geometries. Ideally, instruments would be ready-to-go, packed in suitcases.

Further technical improvements are possible. Instruments are more safely deployed when they can rely on both airplane power and battery power, including the recording devices. Just under 1 Ampere of electric current (110 V / 60 Hz) was available at each window. The biggest technical difficulty in this mission was to provide timing information, but suitable instruments can be purchased to avoid this problem. Finally, when observing in daytime conditions, instruments should have inclinometers to help aim towards the initial acquisition direction.

In a future mission, we may hope that some of these activities can be organized in parallel. In many respects, the proposed mission would be similar, including the use of commercial aircraft, commercial pilots, and the need to arrange over flight clearance if the mission is in territorial waters or over land. The source of pre-impact information about the time and location of the pending re-entry was obtained from the same source as would assist an asteroid impact mission. Instrument installation approaches could be similar to those deployed in this mission. Instruments would need to handle a much brighter object.The dark horse will continue to be the required authorizations for over flight and pre-event access to the aircraft, which depend on the specific location and time of the asteroid impact.

VI. Conclusion

The WT1190F re-entry observing campaign proved to be a successful technology demonstration for a future asteroid impact observation campaign. A chartered aircraft was rapidly deployed to the calculated area of impact. The impact location and time were sufficiently accurately known in advance for flight planning purposes. The aircraft was instrumented and detailed imaging and spectroscopic information on the entry were obtained, even in daylight near-noon conditions. This data documented the fragmentation sequence, the light curve as a function of altitude, the compositional properties of the materials, and narrowed down where to find surviving fragments.

The observations provide ground truth for models that study the behavior of space debris entering Earth's atmosphere at relatively high entry speed and angle. The identity of WT1190F is still to be determined.

Acknowledgments

MSO thanks Falcon Aviation of Abu Dhabi for executing this mission. The mission was made possible by support from the United Arab Emirates government. We thank those involved at the UAE Space Agency and the International Astronomical Center for their assistance in organizing the mission. PJ thanks E. H. Teets of NASA AFRC for assistance with weather data. Many observers, including Nick Moskovitz of Lowell Observatory and Eileen and Bill Ryan of Magdalena Ridge Observatory, contributed to improving the astrometric and photometric data of WT1190F on approach to Earth. The mission was executed over the territorial waters of Sri Lanka. We thank Nalin Samarasinha of PSI and the ground-based observers in Sri Lanka for their efforts to support this campaign. RFD thanks Molly Moir and Eric Steinberg, students at Dexter Southfield, for assistance with the data reduction effort. The instrument teams from the SETI Institute and Dexter Southfield were sponsored by the NASA NEOO program (grant NNX14-AR92G), while the University of Stuttgart team was sponsored by ESA. Part of the research was conducted at the Jet Propulsion Laboratory, California Institute of Technology, under a contract with NASA.

References

[1] Popova, O. P., Jenniskens, P., Emel'yanenko, V., et al., "Chelyabinsk: Airburst, Damage Assessment, Meteorite Recovery, and Characterization," *Science*, Vol. 342, 2013, pp. 1069–1073.

[2] Brown, P., Assink, J. D., Astiz, L., et al., "A 500-kiloton Airburst over Chelyabinsk and an Enhanced Hazard from Small Impactors," *Nature*, Vol. 503, 2013, pp. 238–241.

[3] Brown, P., Spalding, R. E., ReVelle, D. O., Tagliaferri, E., Worden, S. P., "The Flux of Small Near-Earth Objects Colliding with the Earth," *Nature*, Vol. 420, 2002, pp. 294–296.

[4] Veres, P., Farnocchia, D., Jedicke, R., Spoto, F., "The Effect of Parallax and Cadence on Asteroid Impact Probabilities and Warning Times," *Publ. Astron. Soc. Pacific*, Vol. 126, No. 939, 2014, pp. 433–444.

[5] Jenniskens, P., Shaddad, M. H., Numan, D., et al., "The Impact and Recovery of Asteroid 2008 TC3," *Nature*, Vol. 458, No. 26, 2009, pp. 485–488.

[6] Borovicka, J., Charvát, Z., "Meteosat Observations of the Atmospheric Entry of 2008 TC3 over Sudan and the Associated Dust Cloud," *Astron. Astrophys.*, Vol. 507, 2009, pp. 1015–1022.

[7] Chesley, S. R., Farnocchia, D., Brown, P. G., Chodas, P. W., "Orbit Estimation for Late Warning Asteroid Impacts: The Case of 2014 AA," *2015 IEEE Aerospace Conference*, 7–15 March, 2015, Big Sky, MT, Publisher: IEEE, pp. 1–8, doi: 10.1109/AERO.2015.7119148.

[8] Liu, Y., Prabhu, D., Trumble, K. A., Saunders, D., Jenniskens, P., "Radiation Modeling for the Reentry of the Stardust Sample Return Capsule," *AIAA Journal of Spacecraft and Rockets, Vol.* 47, 2010, pp. 741–752.

[9] Trumble, K. A., Cozmuta, I., Sepka, S., Jenniskens, P., Winter, M., "Postflight Aerothermal Analysis of Stardust Sample Return Capsule," *AIAA Journal of Spacecraft and Rockets, Vol.* 47, 2010, pp. 765–774.

[10] Boyd, I. D., Jenniskens, P., "Modeling of Stardust Entry at High Altitude, Part 2: Radiation Analysis," *AIAA Journal of Spacecraft and Rockets, Vol.* 47, 2010, pp. 901–909.

[11] Wercinski, P. F., Jenniskens, P., "Digital Still Snapshots of the Stardust Sample Return Capsule Entry," *AIAA Journal of Spacecraft and Rockets*, Vol. 47, 2010, pp. 889–894.

[12] Jenniskens, P., "Observations of the Stardust Sample Return Capsule Entry with a Slitless Echelle Spectrograph," *AIAA Journal of Spacecraft and Rockets*, Vol. 47, 2010, 718–735.

[13] Farnocchia, D., Chesley, S. R., Micheli, M., "Systematic Ranging and Late Warning Asteroid Impacts," Icarus, Vol. 258, 2015, pp. 18–27.

[14] Pravec, P., Harris, A. W., "Binary Asteroid Population. 1. Angular Momentum Content," *Icarus*, Vol. 190, 2007, pp. 250–259.

[15] Loehle, S., Jenniskens, P., "High Resolution Spectroscopy of the Hayabusa Re-Entry using Fabry-Perot Interferometry," *AIAA Journal of Spacecraft and Rockets*, Vol. 51, 2014, pp. 1986–1993.

[16] Koppenwallner, G., Fritsche, B., Lips, T., Klinkrad, H., "SCARAB - A Multi-disciplinary Code for Destruction Analysis of Space-Craft during Re-Entry," *ESA SP*, Vol. 563, 2005, pp. 281–287.

[17] Roberston, D. K., "Asteroid Defense Modeling," Presentation at *Applied Modeling & Simulation (AMS) Seminar Series.* NASA Ames Research Center, October 14, 2014, pp. 1–30.

[18] Jenniskens, P., Butow, S., "Successful Leonid Airborne Mission," *WGN, the Journal of the IMO, Vol.* 26, 1998, pp. 249–252.

[19] Jenniskens, P., "The 2002 Leonid MAC Airborne Mission: First Results," *WGN, Journal of the IMO*, Vol. 30, 2002, pp. 218–224.

[20] Jenniskens, P., Hatton, J., "An Airborne Observing Campaign to Monitor the Fragmenting Fireball Re-Entry of ATV-1 "Jules Verne" in August 2008," In: *Asteroids, Comets, Meteors 2008*, July 14-18, 2008, Baltimore, Maryland, LPI Contribution No. 1405, 2008, paper id. 8202.

[21] Grinstead, J. H., Jenniskens, P., Cassell, A. M., Albers, J., Winter, M. W., "Airborne Obervations of the Hayabusa Sample Return Capsule Re-Entry," In: *42nd AIAA Thermophysics Conference*, 27–30 June 2011, Honolulu, Hawaii, 2011.

[22] Pavlenko, Ya. V., "Molecular Bands in the Spectra of M Stars," *Astronomy Reports*, Vol. 58, 2014, pp. 825–834.